Behavioral/Cognitive

Feeling of Ownership over an Embodied Avatar's Hand Brings About Fast Changes of Fronto-Parietal Cortical Dynamics

Elias Paolo Casula,[1,2] **Gaetano Tieri,**[3] **Lorenzo Rocchi,**[2,4] **Rachele Pezzetta,**[5] **Michele Maiella,**[1,6] **Enea Francesco Pavone,**[7] **Salvatore Maria Aglioti,**[8,9] **and Giacomo Koch**[1,10]

[1]Non-invasive Brain Stimulation Unit, IRCCS Santa Lucia Foundation, Rome 00179, Italy, [2]Department of Clinical and Movement Neurosciences, UCL Queen Square Institute of Neurology, University College London, London WC1N 3BG, United Kingdom, [3]Virtual Reality Lab, Unitelma Sapienza of Rome, Rome 00161, Italy, [4]Department of Medical Sciences and Public Health, University of Cagliari, Cagliari 09124, Italy, [5]Brain Imaging and Neural Dynamics Research Group, IRCCS San Camillo Hospital, Venice 30126, Italy, [6]Department of Systems Medicine, University of Rome Tor Vergata, Rome 0133, Italy, [7]Applied Neuroscience, BrainTrends ltd, Rome 00179, Italy, [8]Social Neuroscience Lab, IRCCS Santa Lucia Foundation, Rome 00179, Italy, [9]CN2LS@Sapienza at Istituto Italiano di Tecnologia, Sapienza University of Rome, Rome 00161, Italy, and [10]Department of Neuroscience and Rehabilitation, Section of Human Physiology, University of Ferrara, Ferrara 44121, Italy

When we look at our body parts, we are immediately aware that they belong to us and we rarely doubt about the integrity, continuity, and sense of ownership of our body. Despite this certainty, immersive virtual reality (IVR) may lead to a strong feeling of embodiment over an artificial body part seen from a first-person perspective (1PP). Although such feeling of ownership (FO) has been described in different situations, it is not yet understood how this phenomenon is generated at neural level. To track the real-time brain dynamics associated with FO, we delivered transcranial magnetic stimuli over the hand region in the primary motor cortex (M1) and simultaneously recorded electroencephalography (EEG) in 19 healthy volunteers (11 male/8 female) watching IVR renderings of anatomically plausible (full-limb) versus implausible (hand disconnected from the forearm) virtual limbs. Our data show that embodying a virtual hand is temporally associated with a rapid drop of cortical activity of the onlookers' hand region in the M1 contralateral to the observed hand. Spatiotemporal analysis shows that embodying the avatar's hand is also associated with fast changes of activity within an interconnected fronto-parietal circuit ipsilateral to the brain stimulation. Specifically, an immediate reduction of connectivity with the premotor area is paralleled by an enhancement in the connectivity with the posterior parietal cortex (PPC) which is related to the strength of ownership illusion ratings and thus likely reflects conscious feelings of embodiment. Our results suggest that changes of bodily representations are underpinned by a dynamic cross talk within a highly-plastic, fronto-parietal network.

Key words: brain dynamics; EEG; embodiment; TMS

Significance Statement

Observing an avatar's body part from a first-person perspective (1PP) induces an illusory embodiment over it. What remains unknown are the cortical dynamics underpinning the embodiment of artificial agents. To shed light on the physiological mechanisms of embodiment we used a novel approach that combines noninvasive stimulation of the cortical motor-hand area and whole-scalp electroencephalographic (EEG) recordings in people observing an embodied artificial limb. We found that just before the illusion started, there is a decrease of activity of the motor-hand area accompanied by an increase of connectivity with the parietal region ipsilateral to the stimulation that reflects the ratings of the embodiment illusion. Our results suggest that changes of bodily representations are underpinned by a dynamic cross talk within a fronto-parietal circuit.

Introduction

The strong conviction that we own our body and are in control of its actions is challenged not only by brain lesions but also by changing healthy people multimodal integration of visual and tactile inputs concerning the body. A striking example of induced ownership over an external body part [feeling of

Received Mar. 24, 2021; revised Aug. 31, 2021; accepted Sep. 3, 2021.

Author contributions: E.P.C., G.T., E.F.P., S.M.A., and G.K. designed research; E.P.C., G.T., and M.M. performed research; E.P.C., L.R., R.P., M.M., and E.F.P. analyzed data; E.P.C. wrote the first draft of the paper; E.P.C., G.T., L.R., R.P., M.M., S.M.A., and G.K. edited the paper; E.P.C., S.M.A., and G.K. wrote the paper.

E.P.C. is supported by the European Commision with Marie Sklodowska-Curie Individual Fellowship H2020-MSCA-IF Grant No. 798957. G.K. is supported by the Italian Ministry of Health, The Alzheimer's Drug Discovery Foundation (ADDF), and the BrightFocus Foundation. S.M.A. is supported by the PRIN Grant (Italian Ministry of University and Research, Progetti di Ricerca di Rilevante Interesse Nazionale, Edit. 2017, Prot. 2017N7WCLP). We thank all the participants in the experiment.

The authors declare no competing financial interests.

Correspondence should be addressed to Elias Paolo Casula at elias.casula@gmail.com.

https://doi.org/10.1523/JNEUROSCI.0636-21.2021

Figure 1. The TMS-EEG-IVR setup. During IVR, each participant was instructed to observe a virtual right hand while TMS was applied over (1) the left ($Wrist_{l\text{-}M1}$ condition) or (2) the right ($Wrist_{r\text{-}M1}$) hand M1 representation ($M1_{hand}$) or (3) a right disconnected hand while stimulated over the left $M1_{hand}$ ($noWrist_{l\text{-}M1}$). TMS was constantly monitored through stereotaxic neuronavigation, and cortical activation was continuously recorded with EEG. During IVR, participants were asked to refer whether they start to feel the ownership illusion over the virtual right hand, i.e., SoI. TMS, transcranial magnetic stimulation; EEG, electroencephalography; IVR, immersive virtual reality; M1, primary motor cortex; SoI, start of illusion.

ownership (FO)] is the famous rubber hand illusion (RHI; Botvinick and Cohen, 1998).

Neuroimaging studies suggest that embodiment of an artificial body part is linked to activation of different frontal and posterior areas (Ehrsson et al., 2004). The premotor area (PM) seems to have a prominent role, suggested by the positive correlation between its activation and the strength on the illusory FO and the changes in connectivity dynamics with parietal areas (Kanayama et al., 2017). A causal role of the posterior parietal cortex (PPC) in the RHI has also been suggested by its noninvasive stimulation with transcranial magnetic stimulation (TMS; Kammers et al., 2009; Tsakiris et al., 2008; Grivaz et al., 2017). Interestingly, imaging studies have not investigated the role of the primary motor cortex (M1) in the same context. Corticospinal excitability, tested with motor-evoked potentials (MEPs), have been reported to decrease during RHI (Della Gatta et al., 2016). This has been interpreted as a consequence of the decreased potentiality for action which follows the reduced self-consciousness of the upper limb caused by the RHI (Gallese and Sinigaglia, 2010). Taken together, these studies suggested that (1) during body ownership, a large fronto-parietal network is activated; (2) during the illusory ownership of an external hand, changes of excitability of its motor somatotopic representation might occur. Less information is available on the link between cortical network dynamics and the emergence of embodiment-related illusions. Indeed, neuroimaging techniques do not provide the temporal resolution needed for detecting instantaneous changes of cortical activity. On the other hand, the TMS approach based only on MEPs, does not inform on effective connectivity in the neural network involved in the embodiment process.

Recently, thanks to immersive virtual reality (IVR), it has been possible to elicit FO over virtual body parts and its related vicarious agency (VA), i.e., the feeling that we exert full control over virtual body parts actions (Slater et al., 2008). Indeed, the mere observation in IVR of a human virtual body, seen from a first-person perspective (1PP), induces a strong illusory FO over the observed body part (Tieri et al., 2015a). Here, we built a novel setup based on the combination of TMS and simultaneous electroencephalographic (EEG) recordings in healthy participants immersed in a VR scenario and observing from a 1PP, through a head mounted display, a virtual limb perfectly aligned with their real one. Single-pulse TMS was delivered over the hand representation in the M1 ($M1_{hand}$), while measuring EEG changes over all the scalp (Fig. 1). Previous studies already used EEG to explore the electrophysiological correlates of embodiment (Guterstam et al., 2019); however, the main novelty provided by our TMS-EEG-IVR lies in the possibility to directly assess the brain dynamics underpinning embodiment with a causal and directional approach from the stimulated area to the entire cortex (Ilmoniemi et al., 1997). The EEG activity evoked by TMS, in fact, is a direct measure of the excitability of the stimulated area and of its connections. In addition, by reconstructing the timing of activation, it is possible to differentiate the contribution of different interneuronal populations involved in the TMS-evoked cortical response (Premoli et al., 2014a).

We hypothesized that the ownership illusion over the embodied avatar's hand would induce specific spatiotemporal dynamic changes in cortical excitability of somatotopic M1 representation and of other interconnected areas, within a dedicated fronto-parietal circuit (Blanke et al., 2015). We also expected that this change in excitability would occur closely in time to the start of the illusory ownership over the embodied avatar's hand.

Materials and Methods

Participants

Nineteen healthy volunteers (eight females; age mean ± SD, 27 ± 3 years) were enrolled in the study. They were all right handed (Oldfield, 1971), with normal visual acuity, and were naive to the purpose of the experiment. All subjects gave their written informed consent before the experiment and did not have exclusion criteria for TMS (Rossi et al., 2009). The experimental protocol was approved by the ethics committee of the Santa Lucia Foundation and was conducted in accordance with the ethical standards of the 2013 Declaration of Helsinki. The appropriateness of our sample size was established by a power calculation performed with G*Power software, which indicated that 15 participants would be required to detect an effect with a power of 0.95 and an α level of 0.05. Since the TMS-EEG-IVR approach has been used for the first time in the present work, this estimation was based on previous studies in which EEG was recorded while embodying a virtual avatar in 1PP during conflicting conditions (Pezzetta et al., 2018).

General procedure

Participants were seated in a chair and asked to rest their hands comfortably on a table in front of them. Their upper limbs were covered with a white cloth to avoid vision of the hands. Before the experiment, participants underwent a calibration phase where the avatar's size and the point-of-view were adjusted to individual hand size and position. Then, participants underwent three TMS-EEG-IVR sessions, whose order was counterbalanced across subjects. Each session was composed of three recording blocks, named pre-IVR, IVR, and post-IVR; while pre-IVR and post-IVR did not change across sessions, the IVR block was recorded under three different experimental conditions: a target experimental condition named "$Wrist_{l\text{-}M1}$" and two control conditions named "$noWrist_{l\text{-}M1}$" and "$Wrist_{r\text{-}M1}$." Participants were instructed to focus their attention on a virtual right hand, which could appear connected or disconnected from a virtual right forearm, aligned with the real one, while receiving 160 TMS pulses over the hand representation of the left M1 ($Wrist_{l\text{-}M1}$ and $noWrist_{l\text{-}M1}$ conditions, respectively) or of the right M1 ($Wrist_{r\text{-}M1}$ condition; Fig. 2). The two control conditions, i.e.,

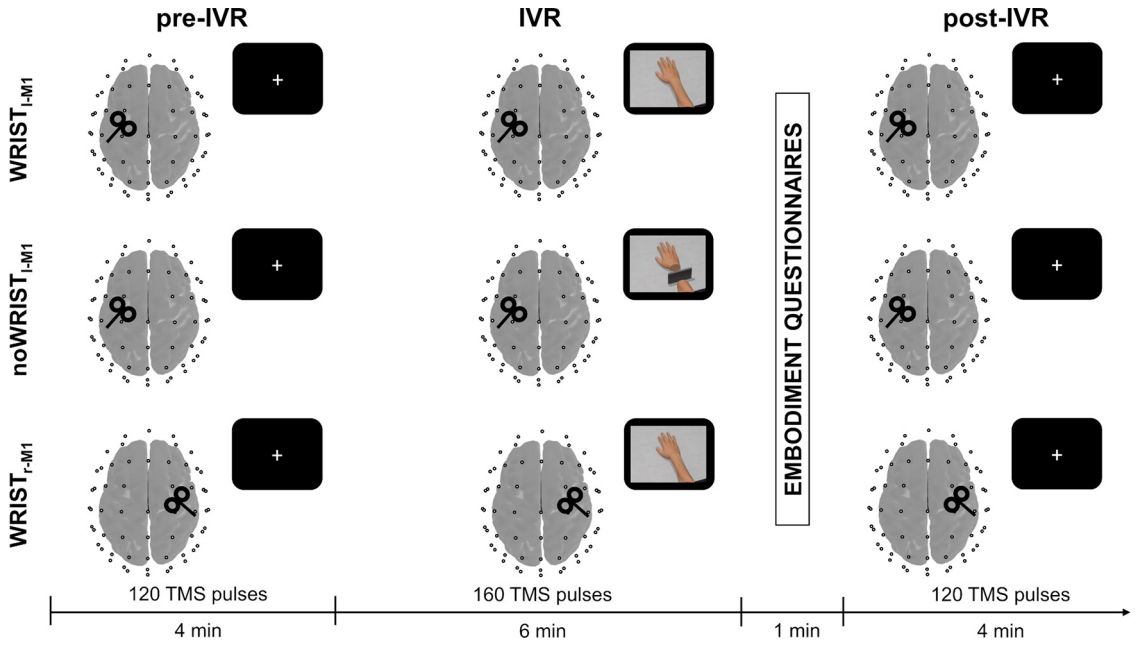

Figure 2. Schematic representation of the experimental procedure. Each participant underwent three TMS-EEG-IVR sessions (one for each condition, i.e., $Wrist_{l\text{-}M1}$, $noWrist_{l\text{-}M1}$, $Wrist_{r\text{-}M1}$), each consisting of an IVR block (160 pulses) preceded by a pre-IVR (120 pulses) and followed by a post-IVR (120 pulses) block. The order of observation conditions was counterbalanced across participants. At the end of IVR block, a black screen covered the whole virtual scenario, and the participants verbally rated the strength of FO and VA over the virtual hand by answering to the embodiment questionnaires. IVR, immersive virtual reality; TMS, transcranial magnetic stimulation; EEG, electroencephalography; M1, primary motor cortex; FO, feeling of ownership; VA, vicarious agency.

$noWrist_{l\text{-}M1}$ and $Wrist_{r\text{-}M1}$, were performed to avoid confounding related to the observed stimulus, i.e., connected versus disconnected arm, and to the site of stimulation, i.e., ipsilateral versus contralateral M1, respectively. During the IVR block, participants were asked to stay still and to report whether they started to feel the illusory ownership over the hand [start of illusion (SoI)] and whether the illusion diminished or disappear [end of illusion (EoI); for more details, see below, Embodiment questionnaire]. Importantly, at the beginning of the experiment, participants were not informed about the different experimental conditions (i.e., appearance of the virtual arm or site of stimulation). At the end of the IVR block, a black screen covered the whole virtual scenario and the participants verbally rated the strength of the FO and VA by answering a questionnaire (see Table 1). During pre-IVR and post-IVR blocks, subjects were asked to fixate a white cross (6×6 cm) in the middle of a black screen, to avoid eye movements, and to maintain a relaxed position, while their upper were covered with a white cloth, to avoid observation of their hands. During both blocks, subjects received 120 TMS pulses over the $M1_{hand}$ hotspot used for the related IVR block. Subjects wore earplugs that played a masking noise reproducing the specific time-varying frequencies of the TMS click to reduce possible auditory responses because of the TMS click (Massimini et al., 2005; Casula et al., 2020), and a 0.5-cm foam layer was place beneath the coil to minimize bone conduction of sound and the sensation caused by coil vibration (Mancuso et al., 2021; Rocchi et al., 2021).

IVR setup

The virtual scenario was designed using 3DS Max 2015 (Autodesk) and implemented in XVR 2.0 (Botvinick and Cohen, 1998; Moseley et al., 2008). It consisted of a dark room with a virtual avatar sitting in front of a real-sized table (scale 1:1). The virtual avatar was created using Poser Pro 2010 library (Smith Micro) and implemented in XVR. The virtual body and the scenario were presented by means of an Oculus Rift DK1 HMD with a 110° field-of-view (diagonal FOV), a resolution of 1280×800 (16:10 aspect ratio, 640×800 per eye) and an internal sensor for head tracking (3 df). The virtual body was presented with the right upper limb placed on the table in a fixed position, while the left upper limb was occluded from view by a virtual gray panel. The virtual right upper limb could take two different visual appearances based on the experimental condition, namely a standard full limb ("Wrist" condition) or a limb with a missing wrist and a plastic gray panel placed in the blank space between the hand and the forelimb ("noWrist" condition; Fig. 2). During the IVR block, the virtual scenario was rendered in both the HMD and a computer screen, so that the experimenter could monitor the participant's point of view and ensure that the virtual hand appeared always at the center of their focus of attention.

Embodiment questionnaire

In order to assess the degree to which participants experienced the illusory FO and VA over the virtual right hand, a 12-item questionnaire (see Table 1) was used. The questionnaire consisted of two parts containing six items, of which three were control items, concerning the FO (Q1–3 experimental, Q4–6 control) and VA (Q7–9 experimental, Q10–12 control), respectively. While the order of the parts was counterbalanced across participants, the order of the items in each part was randomized. Moreover, a vocal reaction time was recorded to determine the exact timing of the SoI and EoI. Specifically, participants were given the following instructions as they observed the virtual hand: "please say 'now' when you begin to feel the virtual hand as your own" (statement adapted from Q3). The average values of Q1–Q3 and Q4–Q6 were considered as an experimental and control index for FO, while those of Q7–Q9 and Q10–Q12 were considered as an experimental and control index for VA.

TMS

TMS was conducted using a Magstim R^2 stimulator with a 50-mm figure-of-eight coil (Magstim Company Limited), which produced a biphasic waveform with a pulse width of ~0.1-ms duration. For $M1_{hand}$ stimulation, the position of the coil on the scalp was functionally defined as the site where TMS evoked the largest MEPs in the relaxed first dorsal interosseous (FDI) muscle of the contralateral hand. This position was sampled in a Montreal Neurologic Institute (MNI) space template

Table 1. Demographic information, RMT of the two hemispheres, SoI, and EoI timings expressed in seconds for each participant in each experimental condition

	Demographic		RMT		Wrist l-M1		noWrist l-M1		Wrist r-M1	
Subject	Age	Sex	l-M1	r-M1	SoI	EoI	SoI	EoI	SoI	EoI
1	25	F	84	88	70				78	
2	25	M	71	71	40				42	
3	25	M	84	85	46				47	
4	26	M	64	72	42				82	
5	32	M	65	79	22		50	110	76	
6	23	F	79	75	86				44	
7	26	M	64	70	43		44		20	
8	28	M	72	64	48				44	
9	24	F	46	49	38				38	
10	30	F	69	73	44				40	
11	32	M	59	60	62				46	
12	27	F	71	72	52				60	
13	32	M	66	72	24				24	
14	24	M	56	67	45				30	
15	26	M	69	63	14		46	86	48	
16	26	F	56	64	30		70	103	18	
17	22	M	65	69	47				84	
18	26	F	53	55	98				62	
19	25	F	52	53	21		48		12	
Avg	26.53		65.53	68.47	45.89		51.60	99.67	47.11	
SE	0.69		2.38	2.31	4.92		4.71	7.13	5.01	

RMT, resting motor threshold; M1, primary motor cortex; SoI, start of illusion; EoI, end of illusion.

derived from a standard 1-mm resolution brain (Colin27). To ensure the same coil positioning throughout the blocks we used a Softaxic neuronavigation system (E. M. S.) coupled with a Polaris Spectra optical measurement system (Northern Digital Inc). During the experimental sessions, the coil was oriented tangentially to the scalp at ~45° away from the midline, so that a posterior to anterior directed current was induced in the brain. Stimulation intensity was 90% of the resting motor threshold (RMT), measured for each hemisphere, and defined as the lowest TMS intensity which evoked at least five out of ten MEPs with a peak-to-peak amplitude of at least 50 μV in the contralateral FDI at rest (Rossini et al., 1994). RMT was re-tested right before all the pre-IVR blocks, to assess whether changes in cortical excitability occurred we performed a one-way ANOVA comparing the RMT among the three conditions ($Wrist_{l\text{-}M1}$, $noWrist_{l\text{-}M1}$, $Wrist_{r\text{-}M1}$). Single pulses were delivered with an average interstimulus interval (ISI) of 2 ± 20% s. Surface EMG was acquired from the right FDI muscle via Ag/AgCl electrodes in a belly-tendon montage and monitored by Signal software (Cambridge Electronic Design). Raw signals were sampled at 2.5 kHz and bandpass filtered between 5 and 1000 Hz. EMG activity from both hands was continuously monitored to ensure that during the experimental session participants kept their hands relaxed and TMS did not evoke any MEPs.

EEG recordings and preprocessing

EEG was recorded using a TMS-compatible DC amplifier (BrainAmp MR plus, BrainProducts GmbH). The amplifier was optically connected to a PC with BrainVision Recorder, through which the EEG was monitored online, and to a 64-channels EEG cap (EasyCap Inc.). EEG was continuously recorded with 62 TMS-compatible Ag/AgCl passive pellet electrodes mounted on the cap according to the 10–20 international system, including Fp1, Fpz, Fp2, AF7, AF3, AF4, AF8, F7, F5, F3, F1, Fz, F2, F4, F6, F8, FT7, FC5, FC3, FC1, FC2, FC4, FC6, FT8, T7, C5, C3, C1, Cz, C2, C4, C6, T8, TP7, CP5, CP3, CP1, CPz, CP2, CP4, CP6, TP8, P7, P5, P3, P1, Pz, P2, P4, P6, P8, PO7, PO3, POz, PO4, PO8, O1, Oz, O2. Recordings were on-line referenced to the tip of the nose and the ground electrode was placed on AFz. Skin impedance was kept below 5 kΩ. EEG signal was bandpass filtered between 0.1 and 1000 Hz and the sampling frequency was 5000 Hz. We first removed the TMS-pulse between −1 and +10 ms, and applied a cubic interpolation on the missing segment. The continuous EEG signal was then bandpass filtered between 1 and 80 Hz (Butterworth zero phase filter). A 50 Hz notch filter was also applied to reduce electrical line noise. After this, the continuous EEG signal was downsampled to 1000 Hz and segmented into epochs starting 1000 ms before the TMS pulse and ending 1000 ms after it. Then, a demean was applied to all the epochs (i.e., the average amplitude of the entire epoch was subtracted from each time point in the epoch), which were then visually inspected, and those with excessive noise were excluded from the analysis (<5% for each participant). Independent component analysis (INFOMAX-ICA) was applied to the segmented EEG signal to identify components reflecting continuous muscle activity, eye movements, blink-related activity, and residual TMS-related artefacts (because of activation of scalp muscles and voltage decay). Artefact-related components were identified in terms of scalp distribution, frequency, timing and amplitude, and then manually removed (Casula et al., 2017). Importantly, during ICA, the three blocks (i.e., pre-IVR, IVR, and post-IVR) were concatenated to ensure that the same artifact-related components were removed, to avoid biasing the results.

Cortical dynamics analysis

EEG analysis was performed with EEGLAB 13.3.2 (Delorme and Makeig, 2004) and Brainstorm toolbox (Tadel et al., 2011), running in a MATLAB environment (version 2017, MathWorks Inc.). To assess cortical excitability changes related to the embodied avatar's hand we first computed TMS-evoked potentials (TEPs) over all the recording electrodes by averaging all the epochs of each block of stimulation. TEPs represent a direct measure of cortical excitability being produced by a mixture of inhibitory and excitatory postsynaptic potentials mediated by different interneuronal populations (Rogasch and Fitzgerald, 2013; Rocchi et al., 2018). For TEPs analysis, we considered a time window from 100 ms before to 300 ms after the TMS pulse.

To track the timing of cortical activation in relation to the perceived FO, we conducted a trial-by-trial analysis before and during the avatar's hand observation (i.e., pre-IVR and IVR block) by means of the ERPIMAGE function, as implemented in EEGLAB. This analysis allowed us to monitor TMS-evoked activity in a millisecond temporal scale and at each trial in relation to the SoI, i.e., the trial at which the participants started to feel the ownership illusion. Trial-by-trial analysis was conducted over a cluster of electrodes surrounding M1 (FC1, FC3, C1, and C3 for left $M1_{hand}$; FC2, FC4, C2, and C4 for right $M1_{hand}$).

To estimate the spatial distribution of cortical activity, we fitted a distributed source model consisting of 8000 elementary current dipoles. These dipole sources were distributed at each vertex of a tessellated cortical mesh template surface derived from a standard 1-mm resolution brain (Colin27) in the MNI space, as provided by Brainstorm toolbox. First, the head model for source imaging was implemented according to the OpenMEEG boundary element method (Gramfort et al., 2010). Based on this head model, the inverse problem was solved using current density maps. Noise covariance for source reconstruction was obtained separately for each subject from a baseline window ranging from 500 to 10 ms before TMS. The estimated source distribution was averaged across all the participants and three regions of interest (ROIs) were chosen a priori to analyze the source activity in a time window from −100 to 300 ms after TMS: hand representation in the M1 ($M1_{hand}$), ventral premotor cortex (PM), and PPC. $M1_{hand}$ ROI was established based on each stimulated hotspot of the 19 subjects tested and was centered over the following MNI coordinates: $x = -44.4 \pm 4$, $y = -14.6 \pm 2$, $z = 49.3 \pm 4$ mm. For the left PPC and the left PM, the following MNI coordinates were chosen, respectively: $x = -47.3$, $y = -77.7$, $z = 37.2$ and $x = -54.2$, $y = 15.7$, $z = 41.5$. These coordinates were selected according to the definition of the Desikan–Killiany atlas (Desikan et al., 2006) and roughly correspond to the coordinates localized from the individual motor hotspot, based on previous neuroimaging and TMS studies for PM (Fink et al., 1997; Bäumer et al., 2009; Buch et al., 2010; Casula et al., 2018) and PPC (Koch et al., 2007; Casula et al., 2016a, b). Basing on previous studies and on our signal-to-noise ratio (on average 5.24), we estimated a localization error (<2 cm) sufficient to discriminate the activations of the three ROIs (Hauk et al., 2019; Samuelsson et al., 2021).

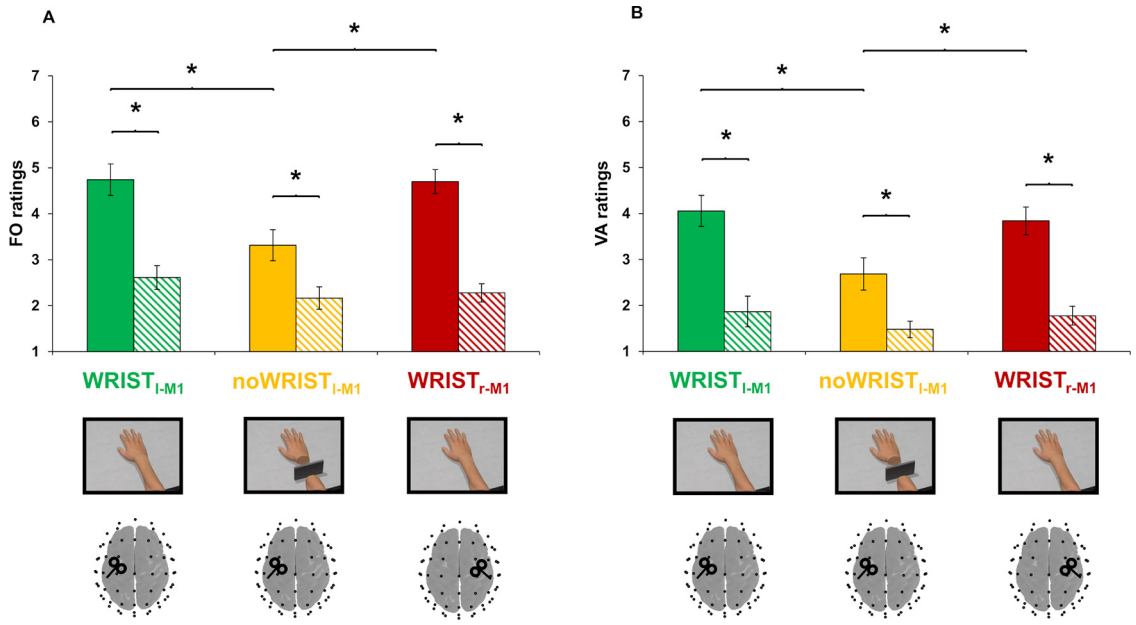

Figure 3. Embodiment measures. Mean ratings of FO (panel ***A***) and VA (panel ***B***) for the $Wrist_{l\text{-}M1}$ (green bars), $noWrist_{l\text{-}M1}$ (yellow bars), and $Wrist_{r\text{-}M1}$ (red bars) condition. Striped bars depict the control items; *$p < 0.05$. Error bars indicate SE. FO, feeling of ownership; VA, vicarious agency; M1, primary motor cortex.

Experimental design and statistical analysis

All data were analyzed using SPSS version 22 (SPSS Inc.) for parametric ANOVA procedures or MATLAB (version 2017, MathWorks Inc.) for nonparametric permutation analysis. Normal distribution of data was assessed by means of the Shapiro–Wilk test. Sphericity of the data were tested with Mauchly's test. Level of significance was set at $\alpha = 0.05$. When sphericity was violated the Greenhouse–Geisser correction was used. Pairwise comparisons were corrected with the Bonferroni method.

Analysis of FO and VA ratings was separately conducted with a two-way ANOVA with factors "condition" ($Wrist_{l\text{-}M1}$, $noWrist_{l\text{-}M1}$, $Wrist_{r\text{-}M1}$) and "item" (target vs control). To exclude any effect of expectations about the experimental condition (i.e., appearance of the virtual arm, site of stimulation) on the strength of illusion, we compared FO/VA ratings in the experimental versus control items of the first experimental condition, i.e., when participants were not aware of the other conditions. This analysis was conducted with paired *t* tests for each single participant tested in the first experimental session (six participants for $Wrist_{l\text{-}M1}$ and $Wrist_{r\text{-}M1}$ condition, seven participants for no $Wrist_{l\text{-}M1}$ condition). Given the high number of *t* test conducted, we used the Bonferroni correction to reduce the occurrence of Type I error ($p_{crit} = 0.05/19 = 0.0026$).

Analysis of TEPs was performed with a nonparametric, cluster-based permutation statistics conducted at each time point, for each individual electrode. This method performs a nonparametric statistical test by calculating Monte Carlo estimates of the significance probabilities from two surrogate distributions constructed by randomly permuting the two original conditions data for 3000 times. The clusters for permutation analysis were defined as the two (or more) neighboring electrodes in which the statistic value at a given time point exceeded a threshold of $p = 0.01$ (Maris and Oostenveld, 2007). This analysis was conducted by comparing the three blocks (pre-IVR, IVR, and post-IVR) and the three conditions ($Wrist_{l\text{-}M1}$, $noWrist_{l\text{-}M1}$, $Wrist_{r\text{-}M1}$).

Analysis of trial-by-trial activity was performed using the same permutation statistics of TEP analysis. To investigate activity at individual level, we computed the mean TMS-evoked activity over the 10 trials before each individual SoI. The averaged TMS-evoked activity at each individual SoI was then compared among the three blocks (pre-IVR, IVR, post-IVR) of the three conditions ($Wrist_{l\text{-}M1}$, $noWrist_{l\text{-}M1}$, $Wrist_{r\text{-}M1}$) by means of a repeated-measures ANOVA.

Analysis of source activity was conducted in two steps. We first performed a preliminary analysis on the averaged baselines of the two pre-IVR blocks with left M1 stimulation (i.e., $Wrist_{l\text{-}M1}$ and $noWrist_{l\text{-}M1}$ condition) to ensure that we could discriminate the activation of left $M1_{hand}$, left PM, and left PPC ROIs. To this aim, we computed a concordance correlation coefficient (CCC) between source activations of $M1_{hand}$, PM, and PPC to check for possible relations and distinguish the three signals (Kerwin et al., 2018; Rocchi et al., 2021; Mancuso et al., 2021). CCC is a nonparametric coefficient optimally tuned to assess agreement between distributions (Lawrence and Lin, 1989). We computed CCC for M1-PM; M1-PPC and PM-PPC, in two time windows: a pre-TMS baseline time window, as a reference (from 200 to 10 ms before the TMS pulse) and a post-TMS time window (from 10 to 200 ms after the TMS pulse). To check for significant differences, we performed paired *t* tests comparing the pre-TMS versus the post-TMS CCC of each subject in the three couples of signals. Afterwards, we did a second analysis aimed at assess cortical excitability changes during IVR (IVR block) compared with baseline level (pre-IVR block) among the different conditions. To this aim, we performed permutation analysis comparing two surrogate distributions constructed by randomly permuting the original distribution data for 3000 times. Significant time points ($p < 0.05$) were then corrected with the false discovery rate method.

To assess whether the activation of $M1_{hand}$, left PM, and left PPC during the observation of the realistic avatar's hand was linearly related to FO and VA ratings, we computed the Spearman's correlation coefficient. All the *p* values resulting from the correlations were corrected with the Bonferroni method ($p_{crit} = 0.05/3 = 0.016$).

Results

Embodiment measures

All of our participants reported to start feeling the ownership illusion (SoI) between 20 and 90 s of observation of the virtual realistic hand, regardless of the TMS site ($Wrist_{l\text{-}M1}$ condition: 45.89 ± 4.92 s; $Wrist_{r\text{-}M1}$ condition: 47.11 ± 5.01 s; all the measures are expressed as mean $\pm$ SE); only five participants reported the SoI during observation of the disconnected hand ($noWrist_{l\text{-}M1}$ condition: 51.6 ± 4.71 s), and three of them reported EoI within the first 2 min of observation (99.7 ± 7.13 s). Analysis of FO ratings revealed a significant "condition × item" interaction ($F_{(2,36)} = 8.024$; $p = 0.001$; $\eta^2 = 0.308$). *Post hoc* comparisons showed that FO ratings measured by experimental items in the no $Wrist_{l\text{-}M1}$ condition (3.31 ± 0.33) were lower compared with the

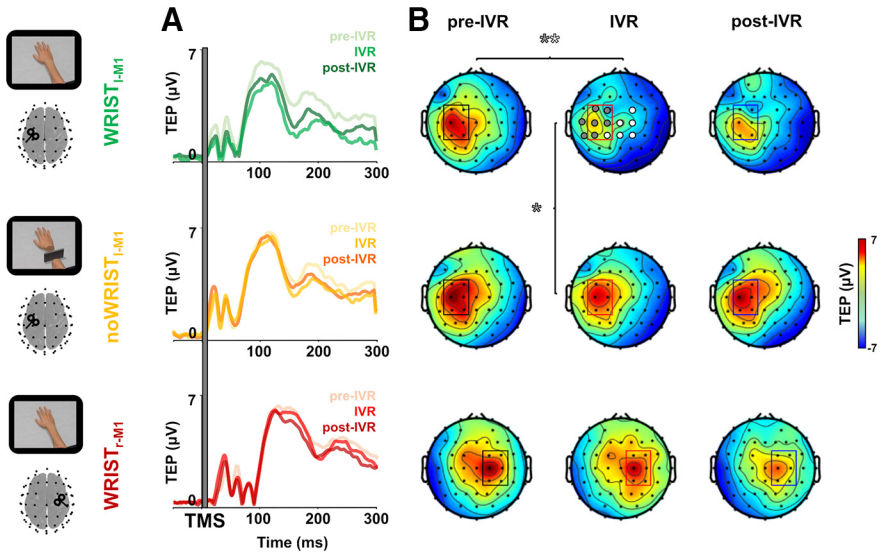

Figure 4. Spatiotemporal analysis of TEPs. TEPs (rectified) from left $M1_{hand}$ for the three sessions ($Wrist_{l\text{-}M1}$, $noWrist_{l\text{-}M1}$, and $Wrist_{r\text{-}M1}$) in the three blocks: pre-IVR, IVR, and post-IVR. (Panel ***A***) Topography of voltage distribution represent TEPs from 40 to 230 ms for all the conditions and in the three blocks. (Panel ***B***) Significant electrodes ($p < 0.05$) from the cluster-based comparison between pre-IVR and IVR block within the $Wrist_{l\text{-}M1}$ session are represented by gray and white circles; significant differences ($p < 0.05$) between the two IVR blocks of the $Wrist_{l\text{-}M1}$ and the $noWrist_{l\text{-}M1}$ conditions are represented by only gray circles. IVR, immersive virtual reality; TMS, transcranial magnetic stimulation; TEP, TMS-evoked potential; M1, primary motor cortex.

$Wrist_{l\text{-}M1}$ condition (4.74 ± 0.34; *post hoc* $p = 0.001$) and to the $Wrist_{r\text{-}M1}$ condition (4.69 ± 0.26; *post hoc* $p = 0.007$; Fig. 3*A*). No significant difference between the target items in the $Wrist_{l\text{-}M1}$ and $Wrist_{r\text{-}M1}$ conditions was found (*post hoc* $p > 0.05$). A main effect of factor item was also observed ($F_{(1,18)} = 102.878$; $p < 0.001$; $\eta^2 = 0.864$), revealing that FO ratings in the control items were the same between conditions (*post hoc* $ps > 0.05$), but were significantly lower compared with target ones (*post hoc* $ps < 0.001$).

Analysis of VA ratings revealed a significant condition × item interaction ($F_{(2,36)} = 4.145$; $p = 0.024$; $\eta^2 = 0.187$). *Post hoc* comparisons showed that VA ratings measured by experimental items in the $noWrist_{l\text{-}M1}$ condition (2.68 ± 0.34) were lower compared with the $Wrist_{l\text{-}M1}$ condition (4.05 ± 0.33; *post hoc* $p = 0.003$) and to the $Wrist_{r\text{-}M1}$ condition (3.84 ± 0.30; *post hoc* $p = 0.043$; Fig. 3*B*). No significant difference between the experimental items in the $Wrist_{l\text{-}M1}$ and $Wrist_{r\text{-}M1}$ conditions was found (*post hoc* $p > 0.05$). A main effect of factor items was also observed ($F_{(1,18)} = 54.439$; $p < 0.001$; $\eta^2 = 0.752$), revealing that VA ratings in control items were the same between conditions (*post hoc* $ps > 0.05$), but were significantly lower compared with target ones (*post hoc* $ps < 0.001$).

Single-subject analysis of FO/VA ratings in the first experimental session, revealed a higher FO/VA ratings in the experimental compared with the control items for each of the six participants tested first in the $Wrist_{l\text{-}M1}$ condition (all $ps < 0.01$; mean $p = 0.0024$), for each of the six participants tested first in the $Wrist_{r\text{-}M1}$ condition (all $ps < 0.01$; mean $p = 0.0008$), whereas none of the seven participants tested first in the $noWrist_{l\text{-}M1}$ condition show any difference between the FO/VA ratings in the experimental versus control items (all $ps > 0.05$, mean $p = 0.259$).

Cortical dynamics

No participants reported any adverse effects because of the stimulation. RMT evaluated with TMS was $65.53 \pm 2.38\%$ and $68.33 \pm 2.37\%$ for the left and right $M1_{hand}$, respectively. When re-tested across sessions, RMT did not change for any of the participants ($p > 0.05$).

Single-pulse TMS of $M1_{hand}$ evoked a well-known sequence of positive and negative deflections in the EEG signal with amplitude ranging from −6 to 6 μV and lasting up to ~250 ms. The cluster-based analysis of TEPs revealed an amplitude reduction over a bilateral cluster of central electrodes during the observation of the realistic avatar's hand, i.e., IVR block of the $Wrist_{l\text{-}M1}$ condition, compared with the pre-IVR and post-IVR block of the same condition ($p < 0.01$; Fig. 4). When the IVR block was compared between conditions ($Wrist_{l\text{-}M1}$ vs $noWrist_{l\text{-}M1}$), differences were significant in a cluster of electrodes in the left stimulated hemisphere ($p < 0.01$; Fig. 4). No differences were observed among the three blocks for the $noWrist_{l\text{-}M1}$ and $Wrist_{r\text{-}M1}$ condition, nor among the pre-IVR blocks of the three conditions (all $ps > 0.05$).

Trial-by-trial analysis revealed a prominent decrease of cortical excitability in the IVR block of the $Wrist_{l\text{-}M1}$ condition between the 12th and the 20th TMS pulse, compared with the pre-IVR block of the same condition and the IVR block of the two control conditions, i.e., $noWrist_{l\text{-}M1}$ and $Wrist_{r\text{-}M1}$ (all $ps < 0.01$); such decrease was still significant at different time windows between the 30th and 90th TMS pulse (all $ps < 0.05$; Fig. 5*A*). To characterize this temporal dynamic at individual level, we measured cortical activity in the significant temporal window for each single participant (Fig. 5*B*). This analysis revealed that, in the $Wrist_{l\text{-}M1}$ condition, 16 out to 19 participants showed a reduction of $42.43 \pm 15.7\%$ of M1-TEP amplitude (pre-IVR block: 5.71 ± 0.45 μV; IVR block: 2.81 ± 0.54 μV), this effect was not observable in the $noWrist_{l\text{-}M1}$ (pre-IVR block: 6.13 ± 0.58 μV; IVR block: 5.96 ± 0.54 μV) nor in the $Wrist_{r\text{-}M1}$ condition (pre-IVR block: 6.09 ± 0.43 μV; IVR block: 6.42 ± 0.47 μV). To verify whether the observed suppression was statistically significant, we conducted a further repeated-measures ANOVA comparing TEP amplitude among the three conditions and the three blocks. This analysis showed a significant condition × block interaction ($F_{(2.36,42.54)} = 8.108$; $p = 0.001$; $\eta^2 = 0.311$). *Post hoc* analysis revealed a significant reduction of TMS-evoked activity during the IVR block of the $Wrist_{l\text{-}M1}$ condition compared with pre-IVR and post-IVR block (all *post hoc* $ps = 0.001$) of the same condition, and compared with all the blocks of the $noWrist_{l\text{-}M1}$ condition (all *post hoc* $ps < 0.01$) and of the $Wrist_{r\text{-}M1}$ (all *post hoc* $ps < 0.001$; Fig. 5*C*). No differences were detected between the pre-IVR blocks of the three conditions (all *post hoc* $ps > 0.9$). In the $Wrist_{l\text{-}M1}$ condition, we observed a decrease of TMS-evoked activity of $42.43 \pm 15.70\%$ during the observation of the realistic avatar's hand; by contrast, in the $noWrist_{l\text{-}M1}$ and in the $Wrist_{r\text{-}M1}$ control conditions, there was an enhancement of TMS-evoked activity, clearer in the $noWrist_{l\text{-}M1}$ condition ($30.26 \pm 27.91\%$) than the $Wrist_{r\text{-}M1}$ condition ($7.04 \pm 4.87\%$).

Source analysis over the three ROIs, i.e., PM, $M1_{hand}$, and PPC, showed three main peaks of activity after the TMS pulse around 30, 100, and 200 ms (Fig. 6*A*). Analysis of CCC showed that pre-TMS signals ($M1_{hand}$-PM: 0.73; $M1_{hand}$-PPC: 0.69; $M1_{hand}$-PPC: 0.59) were significantly higher compared with the post-TMS signals ($M1_{hand}$-PM: 0.14; $M1_{hand}$-PPC: −0.06; $M1_{hand}$-PPC: −0.50; all $ps < 0.05$). During the observation of the realistic avatar's hand, i.e., IVR block of the $Wrist_{l\text{-}M1}$ condition, we found a prominent reduction of PM (from 5 to 32 ms after TMS, mean $p = 0.021$) and $M1_{hand}$ source activity (from 5 to 33 ms after TMS, mean $p = 0.015$) within the first peak of activation, as compared with the baseline level (pre-IVR block), which did not occur in the $noWrist_{l\text{-}M1}$ condition (PM mean $p = 0.529$; M1 mean $p = 0.548$). Differently, we found an opposite pattern for the PPC, in which the neural activity related to the embodiment of the avatar's hand was enhanced within the third peak of activation (from 234 to 268 ms after TMS, mean $p = 0.036$), as compared with baseline level. This effect was not observable in the $noWrist_{l\text{-}M1}$ condition (mean $p = 0.558$).

Analysis of the linear relationships between source activity and embodiment measures, i.e., FO and VA, revealed that FO ratings were directly correlated with PPC source activity during the observation of the virtual realistic hand when embodiment occurred ($R = 0.541$; $p = 0.008$; Fig. 6*B*) whereas the correlation between VA and PPC source activity ($R = 0.389$; $p = 0.050$) did not survive the Bonferroni correction for multiple correlations ($p_{crit} = 0.016$). No significant linear relationships were detected between embodiment measurements and the $M1_{hand}$ or PM source activity (all $ps > 0.05$).

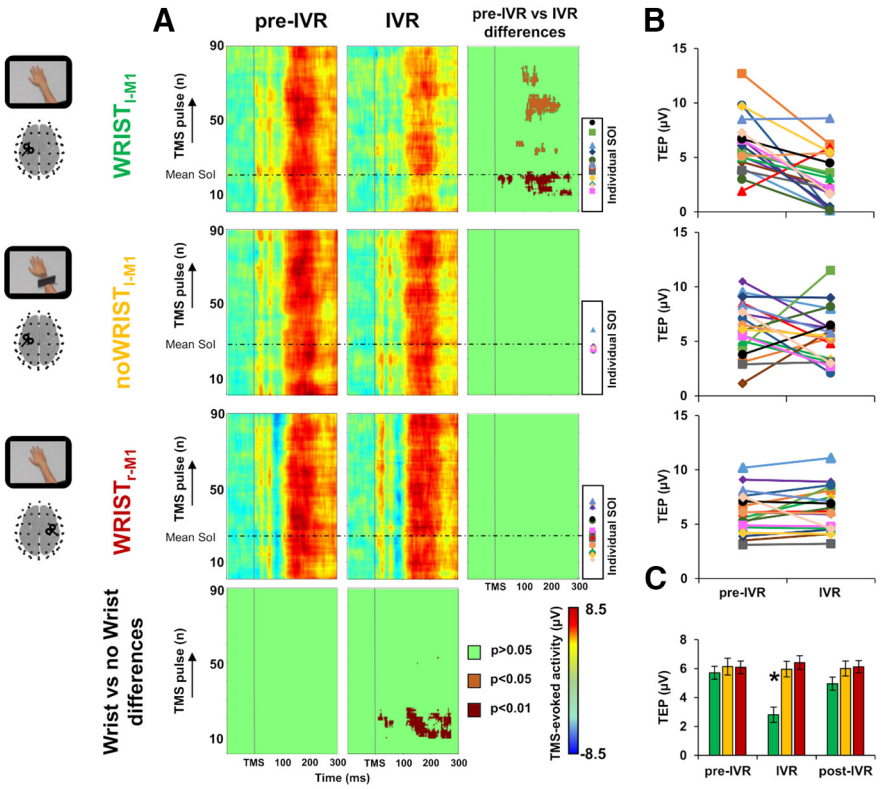

Figure 5. Trial-by-trial analysis. Panel ***A***, Trial-by-trial plots of TMS-evoked activity representing variations in EEG amplitude for the $Wrist_{l\text{-}M1}$, $noWrist_{l\text{-}M1}$, and the $Wrist_{r\text{-}M1}$ condition, in the pre-IVR (left column) and IVR block (central column). The horizontal dotted line represents the average time at which participants started to perceive the illusory ownership of the virtual arm (SoI). Significant differences between blocks (right column) and between conditions (lower row) are depicted in dark red ($p < 0.01$), orange ($p < 0.05$), and green (nonsignificant, $p > 0.05$). Individual SoI are depicted for each participant with a different marker. Panel ***B***, TEP amplitude for each participant in the SoI time window for the $Wrist_{l\text{-}M1}$ condition (upper plot), the $noWrist_{l\text{-}M1}$ (central plot), and the $Wrist_{r\text{-}M1}$ (lower plot). Panel ***C***, ANOVA conducted on the TEP amplitude among the three conditions (green bars, $Wrist_{l\text{-}M1}$; yellow bars, $nowrist_{l\text{-}M1}$; red bars, $Wrist_{r\text{-}M1}$) and the three blocks (pre-IVR, IVR, post-IVR). Error bars indicate SEM; $^*p < 0.05$. IVR, immersive virtual reality; TMS, transcranial magnetic stimulation; M1, primary motor cortex; SoI, start of illusion; EoI, end of illusion.

Discussion

The main contribution provided by our TMS-EEG-IVR study is the physiological characterization of the embodiment-related cortical dynamics. The stimulation of the hand representation in the M1 allowed us to investigate spatiotemporal changes of cortical activity not only within the targeted area (M1) but also in interconnected areas of the fronto-parietal network involved in embodiment processed (PM and PPC). Overall, our data show that FO toward an embodied avatar's hand induces a decrease in contralateral M1 excitability that quickly varies according to changes in the sense of embodiment. During the observation of the realistic avatar's hand, all our participants reported to feel an ownership illusion over the virtual body part. To explore the associated neurophysiological changes in the temporal domain, we measured the cortical activity evoked by each TMS pulse and found a prominent decrease in $M1_{hand}$ excitability in close connection, i.e., a few seconds before the illusion onset (SoI). This effect was observed in 16 out of 19 participants and persisted for the first 3 min of observation after the SoI. Then, we reconstructed the cortical activity in the spatiotemporal domain with a source analysis. We found a decrease of activity in the stimulated $M1_{hand}$ area and in the interconnected PM, within the first 30 ms after the TMS pulse. By contrast, $M1_{hand}$-PPC activation increased around 250 ms after the TMS pulse during the illusory ownership of the avatar's hand. Importantly, this increase was positively correlated with subjective ratings of FO, indicating that participants who reported stronger ownership illusion showed a greater $M1_{hand}$-PPC activation.

Taken together, these results suggest the presence of fast plasticity mechanisms that regulate the neural dynamics within a fronto-parietal network, likely at the basis of the illusory feeling of embodiment of an external body part. Thanks to the accurate timing analysis of the TMS-evoked EEG activity, we could reconstruct the physiological origin of the above dynamics. Early TMS-evoked EEG activity between 10 and 30 ms may reflect glutamate-mediated excitatory post-synaptic potentials (EPSPs), which represent a direct index of excitability (Ferreri et al., 2011; Cash et al., 2017). Differently, later TMS-evoked EEG activity, from 30 to 70 ms and from 70 to 250 ms, may reflect $GABA_A$-mediated and $GABA_B$-mediated inhibitory post-synaptic potentials (IPSPs), as revealed by pharmacological (Kähkönen and Wilenius, 2007; Premoli et al.,

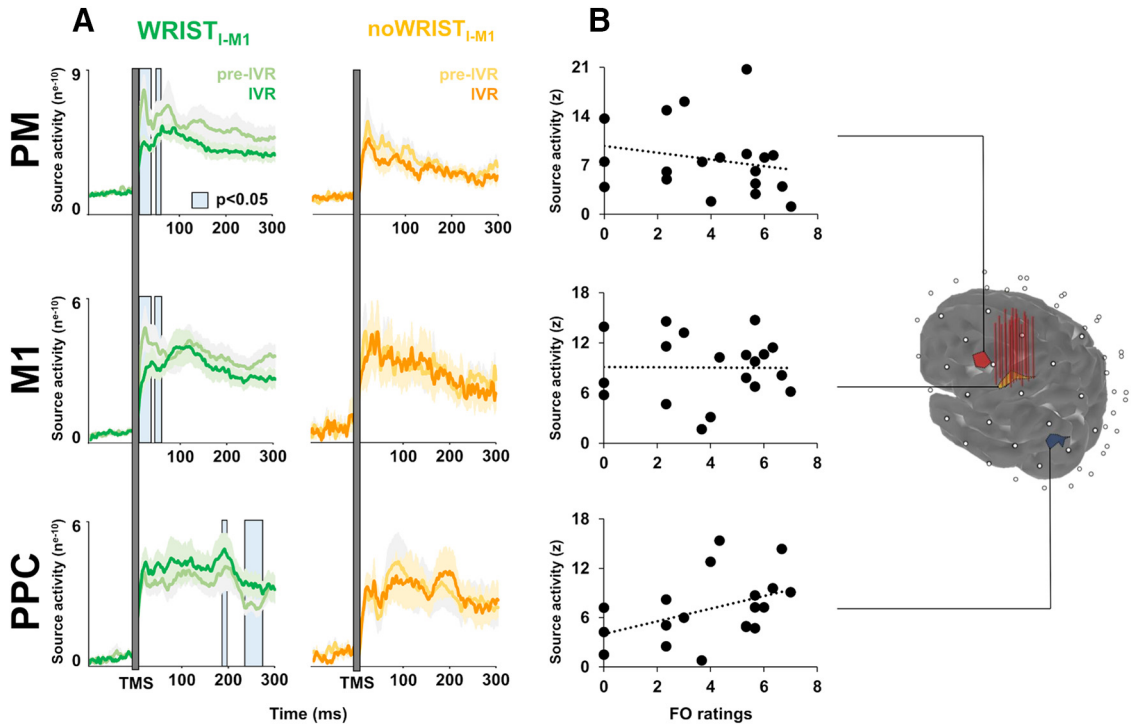

Figure 6. Cortical dynamics in the space domain. Source reconstruction of TMS-evoked activity at ROI level: the stimulated hand area in the M1 ($M1_{hand}$), the PM, and the PPC. Vertical red lines over the $M1_{hand}$ ROI indicate the stimulated hotspot of the 19 participants. Panel ***A:*** timing of the source activity evoked for the $Wrist_{I-M1}$ condition (pre-IVR block, light green line; IVR block, dark green line) and for the $noWrist_{I-M1}$ condition (pre-IVR block, light yellow line; IVR block, dark yellow line). Panel ***B:*** the correlation analysis between source activity of the three ROIs and FO rating. IVR, immersive virtual reality; TMS, transcranial magnetic stimulation; M1, primary motor cortex; PM, premotor cortex; PPC, posterior parietal cortex; FO, feeling of ownership.

2014a,b) and electrophysiological (Daskalakis et al., 2008; Ferreri et al., 2011) studies. In our study, we observed a reduction of early (5–30 ms) TMS-evoked EEG activity both in $M1_{hand}$ and in the interconnected PM, revealing a reduction of excitability in these areas during the ownership illusion of a virtual contralateral hand. On the other hand, we found that late $GABA_B$ergic inhibitory activity (230–270 ms) was enhanced in the $M1_{hand}$-PPC connections. Accordingly, we can speculate that the illusory ownership of an external body part affects the excitability of the motor areas in which the body part is represented. This is probably due to a "substitution" of the real disembodied hand in favor of the virtual embodied one (Della Gatta et al., 2016) along with the prolonged immobility of the hand that could have further reduced its sensorimotor information, thus affecting the motor cortical excitability (Ngomo et al., 2012; Kilteni et al., 2016). From a physiological point of view, we can hypothesize that the reduction in motor excitability is due to a mechanism of GABAergic inhibition originating from the PPC, given the critical role of this area in processing multisensory inputs (Naito et al., 2002; Ehrsson et al., 2005; Grivaz et al., 2017) and given its direct projections to M1 and PM (Koch et al., 2007; 2013). Accordingly, previous studies using a double-coil TMS approach suggested the inhibitory influence of the PPC over corticospinal excitability depending on the strength of RHI (Karabanov et al., 2017; Isayama et al., 2019). This is in line with our correlation analyses showing that participants who experienced a stronger FO illusion were the ones with a higher activation of PPC. Thus, we posit that activity in this parietal region could reflect the conscious feeling of embodiment over the realistic avatar's hand, as previously suggested (Gentile et al., 2013; Preston and Ehrsson, 2016; Lira et al., 2018).

Here, we provide a direct measure of cortical excitability revealing the physiological origin and the timing of the dynamics underlying the feeling of embodiment. By monitoring the TMS-evoked EEG activity trial-by-trial, we could observe that reduction of M1 excitability occurred just a few seconds before the onset of the FO illusion (i.e., SoI). It is worth noting that, to ensure the induction of a reliable illusory FO and VA, we followed a well-established procedure where the feeling of body ownership is induced by passive observation from 1PP in IVR (Tieri et al., 2015a,b; Fusaro et al., 2016; Pezzetta et al., 2018). The present results confirm previous findings concerning the timing and the strength of the illusion (Tieri et al., 2015a,b; 2017; Fusaro et al., 2016; Pezzetta et al., 2018). As matter of fact, all our participants reported the SoI between 20 and 90 s of passive observation of the virtual realistic hand. Notably, embodiment illusion was not affected by TMS itself, nor by the site of stimulation, since participants experienced the same FO and VA both when they were stimulated in the left or right $M1_{hand}$. Tellingly, participants showed a low rate of FO and VA only when they observed the scenario where the virtual hand was disconnected from the virtual forearm and when they responded to the control items, suggesting that the perceived illusion was consistent with the prototypical representation of an intact body (Tieri et al., 2015a,b). In addition, we can exclude a nonspecific effect of the avatar's hand observation that could have influenced cortical excitability (e.g., motor activation, attention fluctuations), since the effects on M1 were observed only when stimulating the $M1_{hand}$ contralateral to the observed virtual hand and not when stimulating the ipsilateral.

Our study has some potential limitations. First, although we could monitor instantaneous changes in cortical excitability during IVR, it was not possible to measure fluctuations in the perceived strength of the FO illusion. To partially overcome this limitation, we asked our participants to report whether the illusion disappeared. In agreement with previous studies using

similar paradigms, none of the participants reported significant changes in the illusion strength during the observation of the realistic avatar's hand (Fusaro et al., 2016; Pezzetta et al., 2018). Our trial-by-trial analysis showed that reduction of cortical excitability persisted for almost 3 min after SoI, although less significantly and discontinuously in time. This could possibly reflect a fluctuation of the FO illusion strength, as observed in a previous study (Kokkinara and Slater, 2014). Second, we could not use individual magnetic resonance imaging (MRI) scans for the source analysis, which was also limited by the relatively low spatial resolution of our EEG recordings. Indeed, it is possible that the $M1_{hand}$-TMS could also have influenced nearby regions. In addition, our source analysis could not discriminate subregions within PM and PPC. To circumvent this potential limitation, we adopted several methodological precautions. First, we used a focal TMS coil (50 mm), checked its location over $M1_{hand}$ based on of MEPs in each participant, and constantly monitored the position using a neuronavigation system. When conducting the source analysis, we computed CCC among the three ROIs activation, revealing a dissociation between signals estimated from different areas. Another limitation lies in the fact that TMS can result in nonspecific effects. Auditory and somatosensory stimulation, for example, may affect the cortical response (Rocchi et al., 2021). To reduce the auditory response, we used an *ad hoc* masking noise; to reduce bone conduction of the TMS click and scalp sensation caused by coil vibration we placed a 0.5 cm foam layer underneath the coil (Casula et al., 2021; Mancuso et al., 2021; Rocchi et al., 2021). It is also important to consider that we tested two control conditions, one related to the observed stimulus (i.e., $noWrist_{l\text{-}M1}$) and one to the site of stimulation ($Wrist_{r\text{-}M1}$). We are thus confident about the specificity of our results.

In conclusion, our data deepen the understanding of the neural mechanisms underlying the FO illusion, in particular in relation to the somatotopic representation of the embodied hand over M1, whose role in embodiment was investigated only with corticospinal measures. Here, we demonstrated that IVR-based embodiment of an avatar's hand elicits rapid changes in cortical excitability that occur just before the ownership illusion of an external body part. Moreover, we provide novel evidence concerning the embodiment-related cortical dynamics within a large fronto-parietal network and showing the timing of activation in a millisecond temporal resolution. The novel TMS-EEG-IVR approach adopted here may allow future investigations of cortical plasticity dynamics underlying physiological and pathologic bodily representation (e.g., hemiplegia, limb apraxia). Moreover, our findings expand our knowledge on the neural bases of embodiment and may be useful to develop novel therapeutic approaches based on IVR in patients with severe motor deficits because of stroke or limb amputation.

References

Bäumer T, Schippling S, Kroeger J, Zittel S, Koch G, Thomalla G, Rothwell JC, Siebner HR, Orth M, Münchau A (2009) Inhibitory and facilitatory connectivity from ventral premotor to primary motor cortex in healthy humans at rest–a bifocal TMS study. Clin Neurophysiol 120:1724–1731.

Blanke O, Slater M, Serino A (2015) Behavioral, neural, and computational principles of bodily self-consciousness. Neuron 88:145–166.

Botvinick M, Cohen J (1998) Rubber hands 'feel' touch that eyes see. Nature 391:756.

Buch ER, Mars RB, Boorman ED, Rushworth MF (2010) A network centered on ventral premotor cortex exerts both facilitatory and inhibitory control over primary motor cortex during action reprogramming. J Neurosci 30:1395–1401.

Cash RF, Noda Y, Zomorrodi R, Radhu N, Farzan F, Rajji TK, Fitzgerald PB, Chen R, Daskalakis ZJ, Blumberger DM (2017) Characterization of glutamatergic and GABA A-mediated neurotransmission in motor and dorsolateral prefrontal cortex using paired-pulse TMS–EEG. Neuropsychopharmacology 42:502–511.

Casula EP, Pellicciari MC, Picazio S, Caltagirone C, Koch G (2016a) Spike-timing-dependent plasticity in the human dorso-lateral prefrontal cortex. Neuroimage 143:204–213.

Casula EP, Pellicciari MC, Ponzo V, Bassi MS, Veniero D, Caltagirone C, Koch G (2016b) Cerebellar theta burst stimulation modulates the neural activity of interconnected parietal and motor areas. Sci Rep 6:36191.

Casula EP, Bertoldo A, Tarantino V, Maiella M, Koch G, Rothwell JC, Toffolo GM, Bisiacchi PS (2017) TMS-evoked long-lasting artefacts: a new adaptive algorithm for EEG signal correction. Clin Neurophysiol 128:1563–1574.

Casula EP, Mayer IM, Desikan M, Tabrizi SJ, Rothwell JC, Orth M (2018) Motor cortex synchronization influences the rhythm of motor performance in premanifest Huntington's disease. Mov Disord 33:440–448.

Casula EP, Maiella M, Pellicciari MC, Porrazzini F, D'Acunto A, Rocchi L, Koch G (2020) Novel TMS-EEG indexes to investigate interhemispheric dynamics in humans. Clin Neurophysiol 131:70–77.

Casula EP, Pellicciari MC, Bonnì S, Spanò B, Ponzo V, Salsano I, Giulietti G, Martino Cinnera A, Maiella M, Borghi I, Rocchi L, Bozzali M, Sallustio F, Caltagirone C, Koch G (2021) Evidence for interhemispheric imbalance in stroke patients as revealed by combining transcranial magnetic stimulation and electroencephalography. Hum Brain Mapp 42:1343–1358.

Daskalakis ZJ, Farzan F, Barr MS, Maller JJ, Chen R, Fitzgerald PB (2008) Long-interval cortical inhibition from the dorsolateral prefrontal cortex: a TMS–EEG study. Neuropsychopharmacology 33:2860–2869.

Della Gatta F, Garbarini F, Puglisi G, Leonetti A, Berti A, Borroni P (2016) Decreased motor cortex excitability mirrors own hand disembodiment during the rubber hand illusion. Elife 5:e14972.

Delorme A, Makeig S (2004) EEGLAB: an open source toolbox for analysis of single-trial EEG dynamics including independent component analysis. J Neurosci Methods 134:9–21.

Desikan RS, Ségonne F, Fischl B, Quinn BT, Dickerson BC, Blacker D, Buckner RL, Dale AM, Maguire RP, Hyman BT, Albert MS, Killiany RJ (2006) An automated labeling system for subdividing the human cerebral cortex on MRI scans into gyral based regions of interest. Neuroimage 31:968–980.

Ehrsson HH, Spence C, Passingham RE (2004) That's my hand! Activity in premotor cortex reflects feeling of ownership of a limb. Science 305:875–877.

Ehrsson HH, Holmes NP, Passingham RE (2005) Touching a rubber hand: feeling of body ownership is associated with activity in multisensory brain areas. J Neurosci 25:10564–10573.

Ferreri F, Pasqualetti P, Määttä S, Ponzo D, Ferrarelli F, Tononi G, Mervaala E, Miniussi C, Rossini PM (2011) Human brain connectivity during single and paired pulse transcranial magnetic stimulation. Neuroimage 54:90–102.

Fink GR, Frackowiak RS, Pietrzyk U, Passingham RE (1997) Multiple nonprimary motor areas in the human cortex. J Neurophysiol 77:2164–2174.

Fusaro M, Tieri SM, Aglioti SM (2016) Seeing pain and pleasure on self and others: behavioral and psychophysiological reactivity in immersive virtual reality. J Neurophysiol 116:2256–2662.

Gallese V, Sinigaglia C (2010) The bodily self as power for action. Neuropsychologia 48:746–755.

Gentile G, Guterstam A, Brozzoli C, Ehrsson HH (2013) Disintegration of multisensory signals from the real hand reduces default limb self-attribution: an fMRI study. J Neurosci 33:13350–13366.

Gramfort A, Papadopoulo T, Olivi E, Clerc M (2010) OpenMEEG: opensource software for quasistatic bioelectromagnetics. Biomed Eng Online 9:45– 20.

Grivaz P, Blanke O, Serino A (2017) Common and distinct brain regions processing multisensory bodily signals for peripersonal space and body ownership. Neuroimage 147:602–618.

Guterstam A, Collins KL, Cronin JA, Zeberg H, Darvas F, Weaver KE, Ojemann JG, Ehrsson HH (2019) Direct electrophysiological correlates of body ownership in human cerebral cortex. Cereb Cortex 29:1328–1341.

Hauk O, Stenroos M, Treder M (2019) EEG/MEG source estimation and spatial filtering: the linear toolkit. In: Magnetoencephalography: from signals to dynamic cortical networks, pp 167–203. Cham: Springer.

Ilmoniemi RJ, Virtanen J, Ruohonen J, Karhu J, Aronen HJ, Näätänen R, Katila T (1997) Neuronal responses to magnetic stimulation reveal cortical reactivity and connectivity. Neuroreport 8:3537–3540.

Isayama R, Vesia M, Jegatheeswaran G, Elahi B, Gunraj CA, Cardinali L, Farnè A, Chen R (2019) Rubber hand illusion modulates the influences of somatosensory and parietal inputs to the motor cortex. J Neurophysiol 121:563–573.

Kähkönen S, Wilenius J (2007) Effects of alcohol on TMS-evoked N100 responses. J Neurosci Methods 166:104–108.

Kammers MP, Verhagen L, Dijkerman HC, Hogendoorn H, De Vignemont F, Schutter DJ (2009) Is this hand for real? Attenuation of the rubber hand illusion by transcranial magnetic stimulation over the inferior parietal lobule. J Cogn Neurosci 21:1311–1320.

Kanayama N, Morandi A, Hiraki K, Pavani F (2017) Causal dynamics of scalp electroencephalography oscillation during the rubber hand illusion. Brain Topogr 30:122–135.

Karabanov AN, Ritterband-Rosenbaum A, Christensen MS, Siebner HR, Nielsen JB (2017) Modulation of fronto-parietal connections during the rubber hand illusion. Eur J Neurosci 45:964–974.

Kerwin LJ, Keller CJ, Wu W, Narayan M, Etkin A (2018) Test-retest reliability of transcranial magnetic stimulation EEG evoked potentials. Brain Stimul 11:536–544.

Kilteni K, Grau-Sánchez J, Veciana De Las Heras M, Rodríguez-Fornells A, Slater M (2016) Decreased corticospinal excitability after the illusion of missing part of the arm. Front Hum Neurosci 10:145.

Koch G, Del Olmo MF, Cheeran B, Ruge D, Schippling S, Caltagirone C, Rothwell JC (2007) Focal stimulation of the posterior parietal cortex increases the excitability of the ipsilateral motor cortex. J Neurosci 27:6815–6822.

Koch G, Ponzo V, Di Lorenzo F, Caltagirone C, Veniero D (2013) Hebbian and anti-Hebbian spike-timing-dependent plasticity of human cortico-cortical connections. J Neurosci 33:9725–9733.

Kokkinara E, Slater M (2014) Measuring the effects through time of the influence of visuomotor and visuotactile synchronous stimulation on a virtual body ownership illusion. Perception 43:43–58.

Lawrence I, Lin K (1989) A concordance correlation coefficient to evaluate reproducibility. Biometrics 45:255–268.

Lira M, Pantaleão FN, de Souza Ramos CG, Boggio PS (2018) Anodal transcranial direct current stimulation over the posterior parietal cortex reduces the onset time to the rubber hand illusion and increases the body ownership. Exp Brain Res 236:2935–2943.

Mancuso M, Sveva V, Cruciani A, Brown K, Ibáñez J, Rawji V, Casula E, Premoli I, D'Ambrosio S, Rothwell J, Rocchi L (2021) Transcranial evoked potentials can be reliably recorded with active electrodes. Brain Sci 11:145.

Maris E, Oostenveld R (2007) Nonparametric statistical testing of EEG-and MEG-data. J Neurosci Methods 164:177–190.

Massimini M, Ferrarelli F, Huber R, Esser SK, Singh H, Tononi G (2005) Breakdown of cortical effective connectivity during sleep. Science 309:2228–2232.

Moseley GL, Olthof N, Venema A, Don S, Wijers M, Gallace A, Spence C (2008) Psychologically induced cooling of a specific body part caused by the illusory ownership of an artificial counterpart. Proc Natl Acad Sci USA 105:13169–13173.

Naito E, Roland PE, Ehrsson HH (2002) I feel my hand moving: a new role of the primary motor cortex in somatic perception of limb movement. Neuron 36:979–988.

Ngomo S, Leonard G, Mercier C (2012) Influence of the amount of use on hand motor cortex representation: effects of immobilization and motor training. Neuroscience 220:208–214.

Oldfield RC (1971) The assessment and analysis of handedness: the Edinburgh inventory. Neuropsychologia 9:97–113.

Pezzetta R, Nicolardi V, Tidoni E, Aglioti SM (2018) Error, rather than its probability, elicits specific electrocortical signatures: a combined EEG-immersive virtual reality study of action observation. J neurophysiol 120:1107–1118.

Premoli I, Castellanos N, Rivolta D, Belardinelli P, Bajo R, Zipser C, Espenhahn S, Heidegger T, Müller-Dahlhaus F, Ziemann U (2014a) TMS-EEG signatures of GABAergic neurotransmission in the human cortex. J Neurosci 34:5603–5612.

Premoli I, Rivolta D, Espenhahn S, Castellanos N, Belardinelli P, Ziemann U, Müller-Dahlhaus F (2014b) Characterization of GABAB-receptor mediated neurotransmission in the human cortex by paired-pulse TMS–EEG. Neuroimage 103:152–162.

Preston C, Ehrsson HH (2016) Illusory obesity triggers body dissatisfaction responses in the insula and anterior cingulate cortex. Cereb Cortex 26:4450–4460.

Rocchi L, Ibáñez J, Benussi A, Hannah R, Rawji V, Casula E, Rothwell J (2018) Variability and predictors of response to continuous theta burst stimulation: a TMS-EEG study. Front Neurosci 12:400.

Rocchi L, Di Santo A, Brown K, Ibáñez J, Casula E, Rawji V, Di Lazzaro V, Koch G, Rothwell J (2021) Disentangling EEG responses to TMS due to cortical and peripheral activations. Brain Stimul 14:4–18.

Rogasch NC, Fitzgerald PB (2013) Assessing cortical network properties using TMS–EEG. Hum Brain Mapp 34:1652–1669.

Rossi S, Hallett M, Rossini PM, Pascual-Leone A (2009) Safety of TMS Consensus Group. Safety, ethical considerations, and application guidelines for the use of transcranial magnetic stimulation in clinical practice and research. Clin Neurophysiol 120:2008–2039.

Rossini PM, Barker AT, Berardelli A, Caramia MD, Caruso G, Cracco RQ, Dimitrijević MR, Hallett M, Katayama Y, Lücking CH, De Noordhout AM (1994) Non-invasive electrical and magnetic stimulation of the brain, spinal cord and roots: basic principles and procedures for routine clinical application. Report of an IFCN committee. Electroencephalogr Clin Neurophysiol 91:79–92.

Samuelsson JG, Peled N, Mamashli F, Ahveninen J, Hämäläinen MS (2021) Spatial fidelity of MEG/EEG source estimates: a general evaluation approach. Neuroimage 224:117430.

Slater M, Pérez Marcos D, Ehrsson H, Sanchez-Vives MV (2008) Towards a digital body: the virtual arm illusion. Front Hum Neurosci 2:6.

Tadel F, Baillet S, Mosher JC, Pantazis D, Leahy RM (2011) Brainstorm: a user-friendly application for MEG/EEG analysis. Comput Intell Neurosci 2011:879716.

Tieri G, Tidoni E, Pavone EF, Aglioti SM (2015a) Body visual discontinuity affects feeling of ownership and skin conductance responses. Sci Rep 5:17139– 17138.

Tieri G, Tidoni E, Pavone EF, Aglioti SM (2015b) Mere observation of body discontinuity affects perceived ownership and vicarious agency over a virtual hand. Exp Brain Res 233:1247–1259.

Tieri G, Gioia A, Scandola M, Pavone EF, Aglioti SM (2017) Visual appearance of a virtual upper limb modulates the temperature of the real hand: a thermal imaging study in immersive virtual reality. Eur J Neurosci 45:1141–1151.

Tsakiris M, Costantini M, Haggard P (2008) The role of the right temporo-parietal junction in maintaining a coherent sense of one's body. Neuropsychologia 46:3014–3018.